

# X-RAY ABSORPTION SPECTROSCOPY AND THE STRUCTURES OF TRANSITION METAL CENTERS IN PROTEINS

C. DAVID GARNER

Department of Chemistry, Manchester University, Manchester M13 9PL, England

- I. Introduction
- II. Theoretical Aspects
- III. Experimental Considerations
- IV. Applications
  - A. Zinc
  - B. Mercury
  - C. Metallothioneins
  - D. Iron Storage and Transport Proteins
  - E. Electron Transfer Centers
  - F. Centers Involved in Oxygen Metabolism
  - G. Oxomolybdoenzymes
  - H. Nitrogenases
- References

## I. Introduction

The appreciation of the significance of bioinorganic chemistry and its dramatic development during the past three decades owes much to the insight, analysis, and scholarship of Professor R. J. P. Williams. Thus, it is now generally acknowledged that metal ions are widely distributed throughout the biosphere and are essential for many of the fundamental chemical transformations necessary to support life (1-4).

The fact that many of the metals are present in biological systems only in trace amounts in no way diminishes their significance. Whenever nature has a difficult task to accomplish, a metal ion (or a cluster of ions) is invariably employed. This is especially true for metabolic processes involving small molecules (3). Thus, the chemical transfor-

mations that constitute the oxygen and nitrogen cycles involve catalyses at transition metal centers. Electron flow in natural systems is overwhelmingly from transition metal center to transition metal center (3). Displacement of charge in biological systems is also achieved by the displacement of alkali and alkaline earth cations, the mobility of which is carefully regulated by ionophores and used to signal, trigger, and control inter- and intracellular processes. Furthermore, Zn(II), Mn(II), and Fe(II) cations are central to the control of both metabolic and genetic processes. Therefore, it is essential that we understand the biochemistry of these metals, especially how the chemistry of a metal is modulated by binding to an organic matrix to achieve a specific functionality. This challenge is clearly manifest by asking *how* symbiosis of transition metal and protein functions produces such elegant specificity (3).

Structural information alone will not describe protein *function*. However, even to ask intelligent questions, it is a prerequisite that we know the detailed structural arrangement of a biomolecule and (in the context of this review) the environment about the transition metal atom.

X-Ray crystallography is rightly regarded as the most powerful structural technique to provide the architectural details of a protein molecule. However, sometimes the resolution of crystallographic data is insufficient to draw meaningful conclusions concerning the detailed nature of a metal center within a protein. Also, some proteins refuse to crystallize or yield crystals suitable for a high-resolution structure determination. Furthermore, it is important to establish structural details for proteins, and especially their catalytic centers, when maintained at conditions similar to their working environment—typically, in aqueous media in the presence of substrate, inhibitor, or suitable redox partner.

In the mid-1970's, with the availability of intense X-ray synchrotron sources, a powerful new technique, X-ray absorption spectroscopy (XAS), emerged. This is a local structural probe, the information content of which derives from electron diffraction. For a metalloprotein, the electron source and detector is the metal atom that is probed, because selective excitation is achieved by scanning a range of X-ray wavelengths particularly appropriate to the element of central interest. The selectivity and the local nature of the diffraction process give the technique its major strength. For example, metal–ligand distances can be determined to an accuracy of approximately  $\pm 0.02$  Å. In addition, XAS does not require crystalline materials; thus, aqueous protein samples are readily probed under a variety of conditions.

Since 1975, when the first experiment using a synchrotron radiation source was accomplished (5), XAS has become established as an important technique for probing the environment of transition metals in proteins. Numerous studies have been accomplished and many significant advances made. The majority of these have been identified and collated in several excellent reviews (6–13), to which readers are referred. This article will provide a qualitative description of the theoretical basis of the technique and outline important experimental considerations, before presenting selected examples of the application of XAS to characterize transition metal centers in proteins.

## II. Theoretical Aspects

The absorption of X rays by a material may be expressed as in Eq. (1),

$$I = I_0 e^{-\mu x} \quad (1)$$

where  $I_0$  is the incident X-ray intensity,  $I$  is transmitted intensity,  $\mu$  is the absorption coefficient; and  $x$  is the thickness of the absorber. Figure 1 contains an illustration of a typical X-ray absorption spectrum, that

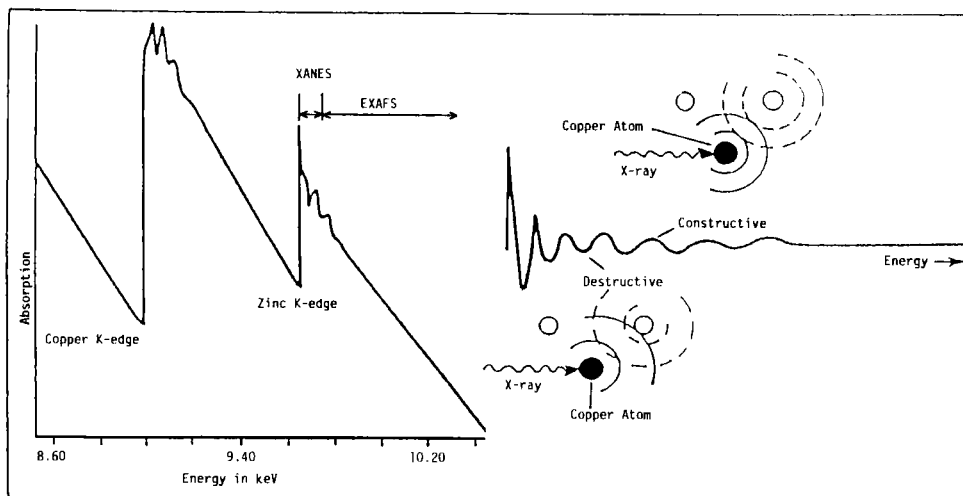


FIG. 1. The X-ray absorption spectrum of Cu,Zn-metallothionein, showing the Cu and Zn K-edges, the demarcation between the X-ray absorption near-edge structure (XANES) and the extended X-ray absorption fine structure (EXAFS), and a pictorial representation of the origin of EXAFS.

for Cu,Zn-metallothionein. For all materials, the generally smooth variation of absorption with increasing photon energy is punctuated by sharp increases in absorption, called absorption edges. These occur at positions where the incident photons are of an energy that is just sufficient to promote an electron from a core level of a particular atom to a valence level and beyond to an unbound state. For a 1s (or K-shell) electron, K-absorption edges result, and Fig. 1 shows the selectivity inherent in the technique, in that the copper and zinc K-edges are clearly resolved. Above the absorption edge,  $\mu$  decreases with increasing photon energy and, apart from gaseous monoatomic species, low-amplitude oscillations are usually observed up to several hundred electron volts above the edge.

Historically, and because of the different theoretical treatment necessary to interpret the data, it has been customary to classify oscillations within  $\sim 50$  eV of the edge as the X-ray absorption near-edge structure (XANES) and those extending beyond this region as the extended X-ray absorption fine structure (EXAFS). The theoretical basis of the latter is considered mature and interpretations of EXAFS data have been reported confidently for over a decade. In contrast, progress in the understanding and, therefore, the application of XANES has been relatively slow and data in this spectral region are generally not interpreted but used qualitatively to "fingerprint" a metal site.

X-ray absorption spectra generally contain two other types of information:

1. The actual energy of a particular absorption edge of an element depends upon the oxidation state and the nature of the immediate chemical environment of that element. Typically, one unit increase of oxidation state increases the energy of the edge position by 1–3 eV. Labhardt and Yuen (14) observed a shift in the position of the iron K-edge and its associated structure of  $\sim 1.5$  eV to higher energy upon oxidation of cytochrome *c*. The sense and magnitude of this shift are consistent with a redox process that is concentrated at the iron center.

2. The excitation of a core electron into the continuum may be convoluted with transitions to the valence levels. These promotions give rise to pre-edge and edge features that can provide information concerning the chemical nature and electronic structure of the primary absorber. Mo=O groups give rise to a low-energy edge inflection due to a transition from the K shell to the Mo=O  $\pi^*$  orbital. This has been a ubiquitous feature of the molybdenum K-edge XAS studies of the oxomolybdoenzymes, as opposed to the nitrogenases (9, 13, 15).

The EXAFS (or XANES) amplitude  $\chi(k)$  is defined as the modulation of the absorption coefficient,  $\mu$ , of a particular atom relative to the smooth background absorption coefficient,  $\mu_s$ , normalized by the absorption coefficient that would be observed for a free atom  $\mu_0$  [Eq. (2)].

$$\chi(k) = (\mu - \mu_s)/\mu_0 \quad (2)$$

Although EXAFS and XANES are recorded as a function of energy, it is conventional to plot the data as a function of  $k$ , the photoelectron wave vector [Eq. (3)]: where  $E$  is the energy of the X-ray photon,  $E_0$  is

$$k = 2\pi/h[2m(E - E_0)]^{1/2} \quad (3)$$

the energy of the absorption threshold,  $m$  is the mass of the electron, and  $h$  is Planck's constant.

Lee and Pendry (16) and Ashley and Doniach (17) showed that, except for the energies very close to the absorption threshold, a single scattering formalism is usually sufficient to describe the observed EXAFS. The effect is shown pictorially in Fig. 1, which depicts a photoelectron being generated by the absorption of an X-ray photon by a copper atom and backscattered from an adjacent atom. As the photon beam energy is smoothly increased beyond the ionization threshold, so the wavelength of the photoelectron decreases and there will be a smooth and continuous movement through constructive, then destructive, then constructive, etc., interference of the outgoing and backscattered waves. Constructive and destructive interference, respectively, increase and lower the absorption coefficient, as compared to the free atom value. When the energy of the photoelectron is sufficiently high, the curvature of the photoelectron wave can be neglected and the theory can be greatly simplified as the plane wave approximation. In this approximation, the oscillatory EXAFS function,  $\chi(k)$ , associated with a K-absorption edge, may be written as Eq. (4):

$$\begin{aligned} \chi(k) = & -\sum_j 3 \cos^2 \theta_j \frac{N_j}{kR_j^2} |f_j(\pi)| \sin(2kR_j + 2\delta_i \\ & + \varphi_j) \exp(-2\sigma_j^2 k^2) \exp(-2R_j/\lambda) \end{aligned} \quad (4)$$

This equation shows the structural basis of EXAFS, in that  $\chi(k)$  is dependent on the following factors:

1. The number of scattering atoms  $N_j$ .
2. The distance of the scattering atoms  $R_j$  from the primary absorber.

3. The type of scattering atom, through the characteristic energy dependence of the backscattering amplitude  $|f_j(\pi)|$ , the magnitude of which generally increases with increasing  $Z$ .
4. The phase shift  $2\delta_j$  due to the potential of the emitting atom.
5. The phase of the backscattering factor  $\varphi_j$ .

The mean square variation in  $R_j$  is represented by the Debye-Waller factor,  $\sigma_j^2$ ;  $\lambda$  is the elastic mean-free path of the photoelectron and it is the damping term  $[\exp(-2R_j/\lambda)]$  that invariably limits backscattering contributions to  $<4 \text{ \AA}$  from a metal atom in a biological system. The  $j$ th neighbor makes an angle  $\theta_j$  with the polarization vector of the incident X ray and the term  $3 \cos^2 \theta_j$  averages to 1 for solutions and polycrystalline samples.

At lower photoelectron energies, the plane wave approximation [Eq. (4)] breaks down and leads to errors in the calculated phase, which in turn can result in an incorrect determination of the interatomic distances. Furthermore, it is this low-energy part of the EXAFS spectrum that usually contains most of the backscattering from the low  $Z$  backscatters and/or more distant shells. This is particularly important in the case of biological systems such as metalloproteins, wherein the range of the EXAFS data is often limited because backscattering is weaker from low  $Z$  atoms and it is the location of atoms such as nitrogen or oxygen that is crucial to many investigations. The low-energy part of the EXAFS spectrum can be analyzed by use of the exact theory given by Lee and Pendry (16), which takes account of the curvature of the electron wave and thus has been named the "spherical wave method." Unfortunately, this exact theory has not been used in a majority of studies due to its mathematical complexity and requirement for large computational time. However, this exact theory has been simplified by performing an average over the angular positions of the scattering atoms relative to the X-ray beam direction (18) and has been consolidated in the Daresbury analysis program EXCURVE. This simplification is strictly only applicable to data analysis for polycrystalline or amorphous samples but is well suited for virtually all studies of transition metals in biological systems.

The first stage in EXAFS data analysis is the removal of the background absorption and the extraction of the EXAFS and its normalization to that for a unit metal atom. An inadequate removal of the background can result in a number of deficiencies in the EXAFS data, which may lead to inaccurate determination of the amplitude function and/or distortions of the low " $R$ " contribution. The EXAFS may be plotted as a function of  $k$ . Often it is convenient to weight the data by

$k^n$  (unusually  $n = 2$  or  $3$ ) to enhance the data at high  $k$ . Figure 2 shows the iron K-edge EXAFS ( $\times k^3$ ) recorded for the iron-molybdenum co-factor (FeMoco) extracted from the FeMo-protein of the nitrogenase of *Klebsiella pneumoniae* (19), together with its Fourier transform.

Sayers *et al.* (20) recognized that the Fourier transform of  $\chi(k)$  would yield a radial distribution function, providing a visual representation of the atomic arrangement about the primary absorber. This peaks at distances close to the corresponding  $R_j$  values [Eq. (4)], the area of the peak depending upon the number of backscattering atoms ( $N_j$ ) within the shell and their backscattering amplitude  $|f_j(\pi)|$ . Unless a correction is applied, the peaks in the Fourier transform occur at a lower  $R_j$  than the actual value, due to the phase shift that the backscattered photoelectron experiences. This was recognized by Sayers *et al.* (20) and they subsequently showed that the phase shift of an absorber and scatterer pair can be extracted from a related compound of known structure and used to obtain an accurate value for the corresponding distance in an unknown system. Alternatively, it is possible to calculate the absorber and backscatterer contributions to the phase shift separately (16). Both of these approaches have been successfully used for structural studies of metal centers in proteins.

EXAFS data analysis consists of varying  $E_0$  and the values of—at least— $R_j$ ,  $N_j$ , and  $\sigma_j$ , for each shell of atoms adjacent to the primary absorber, to produce optimum agreement between the experimental and simulated data and their Fourier transforms.

The level of agreement may be assessed by a fit index FI [e.g., Eq. (5)], summed over all  $n$  points. However, this should not be at the expense of deficiencies obvious from a visual inspection. The level of improvement achieved by addition of an extra shell needs to be carefully monitored and the statistical significance assessed (21).

$$\text{FI} = \sum_{i=1}^n \frac{k^n [\chi_{\text{exp}}(k)^2 - \chi_{\text{th}}(k^2)]}{100n} \quad (5)$$

The major source of uncertainty in parameter determination by EXAFS analysis arises from the correlation that exists between the coordination number ( $N_j$ ) and the Debye-Waller factor ( $\sigma_j^2$ ) for each shell. This correlation occurs through the *amplitude* of the backscattered wave [Eq. (4)] and results in the uncertainty in  $N_j$  being  $\sim \pm 25\%$ . The primary manifestation of  $R_j$  is in the relative *phases* of the outgoing and backscattered waves and, although  $R_j$  is strongly correlated to

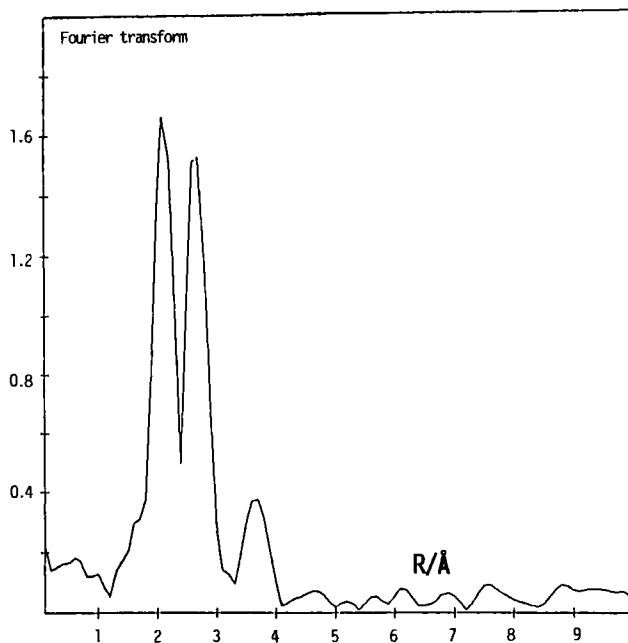
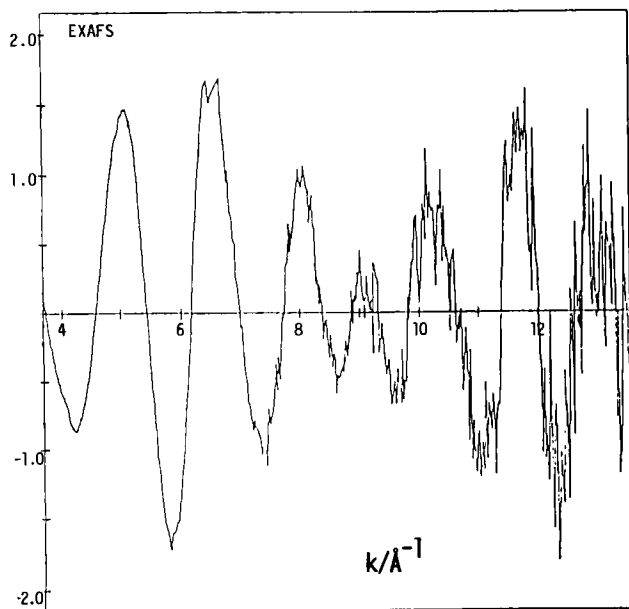


FIG. 2. The  $k^3$ -weighted EXAFS data associated with the iron K-edge of the iron-molybdenum cofactor (FeMoco) extracted from the FeMo-protein of the nitrogenase of *Klebsiella pneumoniae*, and its Fourier transform (19).



$E_0$ , in general  $R_j$  values can be determined to an accuracy of about  $\pm 0.02$  Å. The atomic number of the backscattering atoms cannot usually be determined to a precision better than  $\pm 1$ , because  $|f_j(\pi)|$  and  $\theta_j$  [Eq. (4)] do not show a marked dependence on  $Z$ . The present limitations in the accuracy with which  $N_j$  and  $Z$  values can be determined are especially frustrating for the characterization of metal centers in proteins. Therefore, wherever possible, the information obtained from other spectroscopic and structural techniques should be incorporated into the EXAFS analysis to help remove ambiguity.

Multiple-scattering contributions are generally not important in the EXAFS region. However, this is not so for systems that have colinear arrangements of three or more atoms. For transition metals in biological systems, multiple-scattering effects are very important for  $M-C\equiv O$  and  $M-C\equiv N$  moieties and for coordination by imidazole groups (Fig. 3). Theoretical developments (22) allowing the inclusion of double- and triple-scattering contributions have allowed satisfactory data analyses of multiple-scattering contributions (23). These and other (24) developments are advancing the possibilities of successfully interpreting the XANES region, where extensive multiple scattering of the photoelectron occurs.

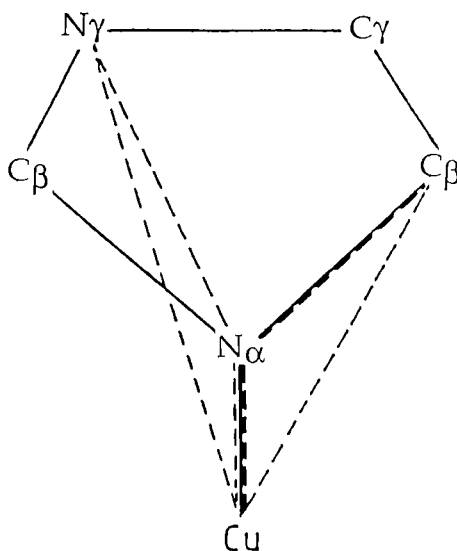


FIG. 3. Representation of copper-imidazole coordination showing the important multiple-scattering pathways.

### III. Experimental Considerations

Within an X-ray absorption spectrum, the signal is generally small compared with the atomic absorption resulting from the excitation of the core electron of the atom of intensity (Fig. 1). Thus good-quality EXAFS and XANES data require an intense and stable X-ray source. To date, there has been no XAS study of a metalloprotein using a laboratory X-ray source such as a rotating anode; all such studies have required synchrotron radiation sources. A recent valuable development at many such facilities has been the inclusion of insertion devices, especially wavelength shifters and multipole wiggler magnets, to increase the intensity available, particularly at shorter wavelengths.

Synchrotron radiation sources, such as the Daresbury SRS, are continuous and intense X-ray sources for the study of the K-edge XAS of elements with  $Z < 65$ . However, there are two limitations to this range:

1. The application of XAS to elements with  $Z < 20$  is limited in many facilities because of the use of beryllium windows on the majority of the X-ray beam lines of synchrotron radiation sources; these are necessary to separate the high vacuum of the source from the experiment, which is normally in air or at poor vacuum. However, by working with the sample in a vacuum, XAS can be recorded for elements down to  $Z \sim 6$ .

2. The large lifetime broadening, due to the limited electron and hole lifetime at high excitation energies, places an upper limit on  $Z$ .

The heaviest element that has been investigated by K-edge EXAFS is iodine ( $Z = 53$ ), which has its K-edge at  $0.37 \text{ \AA}$  (33,500 eV) and has a lifetime broadening of  $>7 \text{ eV}$ . For the higher  $Z$  elements, L-edge XAS can be recorded, concomitant with the excitation of a  $2s$  or  $2p$  electron; typically, L-edge data can be recorded for molybdenum ( $Z = 42$ ) to uranium ( $Z = 92$ ).

The "channel-cut" monochromator is the simplest type employed experimentally. A channel is cut in a perfect crystal (e.g., Si) to provide two parallel reflecting surfaces that have a particular crystal plane [e.g., the Si (220)] parallel to the surface. The Bragg condition is used to select a particular wavelength and the reflected beam emerges parallel to the incident beam but is vertically displaced by  $2D \cos \theta$ , where  $D$  is the distance between the two faces and  $\theta$  is the angle between the beam and the Bragg planes. The accuracy of data collected using channel-cut crystal monochromators may be limited due to harmonic con-

tamination of the reflected beam. Harmonic suppression can be achieved by use of a double-crystal monochromator, which has the two crystal faces slightly offset; this effect is chosen to give a high acceptance of the particular fundamental wavelength ( $\lambda$ ), together with good harmonic rejection of its harmonics ( $\lambda/2$ ,  $\lambda/3$ , . . .).

The conventional XAS experiment involves the direct measurement of the incident and transmitted beam intensity using ionization chambers. The first chamber contains a weakly absorbing gas, which permits  $\leq 70\%$  of the incident radiation to fall on the sample, and the second ionization chamber contains a mixture of inert gases that will absorb virtually all of the transmitted intensity. The measured absorption coefficient comprises that due to the matrix ( $\mu_M$ ) and that due to the atom of interest ( $\mu_A$ ). The application of transmission method is ultimately limited by the incident number of photons and the ratio of  $\mu_M$  to  $\mu_A$ . In cases where  $\mu_M/\mu_A = 1$ , it is difficult to use the transmission method, and for ratios greater than 10 it is almost impossible. The detection sensitivity can be enhanced if a discrimination can be made between the matrix and host absorption. X-Ray fluorescence offers just this possibility. As the fluorescence yield is practically independent of the excitation energy over an EXAFS spectrum ( $\sim 1000$  eV above the edge), a change in the absorption cross-section is directly reflected by a change in the fluorescence yield. This increased contrast arises because the fluorescence of the element of interest, in the region of one of its absorption edges, is considerably greater than that of the lighter, matrix, atoms. Fluorescence detection is now a standard procedure for recording XAS for metal atoms in biological systems. Originally Tl-doped NaI scintillators were employed, but now a new generation of solid-state detectors with improved sensitivity and stability are favored. These allow data to be collected at concentrations  $\leq 1$  mM in the element of interest.

Therefore, XAS—especially with respect to EXAFS—has many advantages as a probe of transition metal centers in biological materials. Beyond the absence of a requirement for crystalline materials, the major attractions are the specificity, and sensitivity of the technique and the provision of interatomic distances with an accuracy of  $\pm 0.02$  Å within (say) 4 Å of the primary absorber. However, it should be noted that (1) no angular information is usually obtained; (2) rarely does the structural information extend beyond 4 Å, (3) the spectrum sums data for all atoms of a particular element and, if the element of interest is present in more than one chemical form, an *average* environment is obtained; (4) the possibility of radiation damage must be anticipated and the integrity of samples should be monitored after, and if possible

during, measurement; and (5) XAS is a "sporting method," and the strength of any interpretation will benefit from other information. As illustrated by studies on rubredoxin (25) and Cu,Zn-superoxide dismutase (26), XAS and protein crystallography are especially complementary.

#### IV. Applications

##### A. ZINC

Zinc is as common as iron in biology and Williams has argued that the role of zinc is vital, not only for catalysis but also in inhibitory control (27). Zinc is now known to be associated with a large variety of proteins (28).

Some crystal structures of zinc proteins are available (29); however, information concerning zinc centers in proteins is rather limited. Because of its filled 3*d*-shell, zinc is not accessible by spectroscopic techniques such as optical absorption and EPR. Zinc sites in proteins may be studied indirectly by spectroscopy; Cd substitution and monitoring by  $^{113}\text{Cd}$  NMR spectroscopy or Co substitution and monitoring by UV-visible or circular dichroism are popular procedures. Nevertheless, it should be borne in mind that these surrogates may not be faithful reporters of zinc sites.

XAS in general, and EXAFS in particular, offer a unique and direct probe of zinc centers in proteins. So far, only three types of amino acid residues have been identified as ligands of zinc in a protein: an imidazole nitrogen of histidine, the carboxylate oxygen of glutamic or aspartic acid, and the sulfur of cysteine. A tentative classification of zinc enzymes based on distinctions possible by EXAFS may be suggested (30):

1. Type A zinc: coordination by sulfur exclusively.
2. Type B zinc: coordination by sulfur and nitrogen and/or oxygen.
3. Type C zinc: coordination by nitrogen and/or oxygen.

The potential of EXAFS to distinguish between types A, B, and C derives from the facts that (1) the backscattering amplitudes of sulfur and nitrogen (or oxygen) are approximately  $\pi$  out of phase when placed at a similar distance from the absorber atom; (2) Zn—S bonds are typically  $\sim 2.3$  Å in length whereas Zn—N/O bonds are  $\sim 0.3$  Å shorter; and (3) the amplitude of sulfur backscattering is significantly greater than that from nitrogen (or oxygen).

Type A and type C centers can be readily distinguished. Type B centers are usually readily identified, but it may be difficult to determine the respective occupancies of the two shells precisely, because the contributions are typically not well resolved in the Fourier transform. Also, it is unfortunate that EXAFS cannot distinguish between carboxylate oxygens and water as ligands of zinc. However, coordination by imidazole is usually clearly evident because of the multiple-scattering pathways involving all atoms of the five-membered ring (23, 26).

Type A zinc sites have been identified in metallothioneins (31) and aspartate transcarbamylase (32). Both involve four sulfur atoms at  $\sim 2.33$  Å from the zinc. Such sites will not be catalytically active, as the coordination sphere of the metal is saturated. Therefore, a function for the zinc as a *pivot*, holding together the regulatory chains of the enzyme in a firm but flexible manner, is proposed (32).

Although type B and type C zinc sites are known to be catalytically active, in these environments zinc can also play an important structural role. This is especially true for "zinc finger proteins." The transcription factor IIIA of eukaryotic cells is a protein with a distinctive repeat sequence, consisting of two cysteine and two histidine residues. These bind zinc in a tetrahedral site, causing a loop or "finger" to be formed (see Fig. 4). The finger binds in the wide groove of DNA in a sequence-specific manner. Thus, the DNA binding capability is controlled by the coordination at the zinc and a similar structural motif has been identified in numerous proteins. Diakun *et al.* (33) showed that zinc in transcription factor IIIA from *Xenopus laevis* is coordinated by two sulfur and two nitrogen atoms (at 2.30 and 2.00 Å, respectively), consistent with ligation by two cysteine and two histidine residues.

The glucocorticoid receptor enhances or represses transcription by binding to specific DNA sequences, termed glucocorticoid response elements. The protein is organized as functional domains, in an ar-

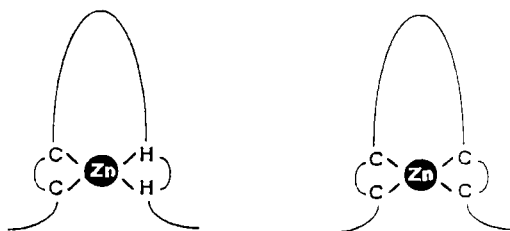


FIG. 4. Representation of the formation of a 2Cys-2His or 4Cys zinc finger protein loop.

rangement that appears to be common among members of the steroid receptor family. A segment near the center of the gene specifies DNA-binding activity *in vitro* and contains two sequence motifs similar to the zinc fingers of transcription factor IIIA. Such sequence motifs have been identified in nucleic acid-binding proteins from a wide range of organisms. Metal ions, notably zinc(II) but also cadmium(II) and cobalt(II), are required for specific DNA binding and proper folding of the protein. The proposal that steroid receptor fingers bind to zinc through two pairs of conserved cysteine residues is consistent with zinc K-edge EXAFS data recorded for the 150-amino acid glucocorticoid receptor fragment that encompasses the DNA-binding region. Zinc is considered to be in a tetrahedral environment, with four Zn—S contacts of  $\sim 2.32$  Å (34).

In a related study (35), the structure of the zinc centers within the DNA-binding domain of the transcriptional activator GAL4, isolated from the yeast *Saccharomyces cerevisiae*, has been investigated by XAS. The amino-terminal DNA-binding domain of the transcription factor contains a metal-binding region, Cys-X<sub>2</sub>-Cys-X<sub>6</sub>-Cys-X<sub>6</sub>-Cys-X<sub>2</sub>-Cys-X<sub>6</sub>-Cys (X = amino acid), which is highly conserved among several other fungal gene regulatory proteins. Circular dichroism spectroscopy suggests that the 149 amino acids are organized as  $\sim 40\%$   $\alpha$ -helix and  $\sim 20\%$   $\beta$ -sheet, and removal of the native zinc(II) causes some unfolding of the secondary structure. A comparative study of the zinc(II) and cadmium(II) proteins was undertaken because this allowed the information available from <sup>113</sup>Cd NMR spectroscopy (36) to complement the EXAFS data analysis.

The zinc K-edge XANES profile of Zn(II) GAL4 is very similar to that of [NEt<sub>4</sub>]<sub>2</sub>[Zn(SPh)<sub>4</sub>], in which zinc is tetrahedrally coordinated by four sulfur atoms (37), zinc in metallothionein (30), and the DNA-binding domain of the glucocorticoid receptor (34). However, the EXAFS associated with the zinc K-edge can best be simulated by backscattering from three sulfur atoms at 2.30 Å, a single oxygen (or nitrogen) atom at 1.96 Å, and a sulfur atom at 3.34 Å. Analytical data suggest that GAL4 has two metal-binding sites per molecule and thus the EXAFS data can be interpreted in one of two ways. First, each zinc might be coordinated by three sulfur-donor ligands and a single oxygen-donor (or nitrogen-donor) ligand. Alternatively, one zinc might be coordinated by four sulfur-donor ligands and the other by two sulfur-donor ligands and two oxygen-donor (or nitrogen-donor) ligands. XAS alone cannot distinguish between these two possibilities.

<sup>113</sup>Cd NMR spectroscopy (36) shows clear evidence for two metal-binding sites within GAL4; one gives rise to a resonance at 707 ppm,

consistent with coordination to four sulfur-donor ligands, the other produces a resonance at 669 ppm, perhaps indicative of coordination by a smaller number of sulfurs. However, the cadmium K-edge EXAFS is well interpreted with four sulfur atoms at 2.47 Å from the metal. Because GAL4 contains only six cysteinyl residues within its DNA-binding domain, the cadmium center may involve at least one bridging cysteine. Given the similar DNA binding affinity, it would be expected that the structure of Zn(II) GAL4 would be the same as that of the Cd(II) protein. The EXAFS data do not favor this conclusion, but it is possible that both the oxygen ligand and the sulfur atom at 3.34 Å are due to the displacement of one or more of the cysteines coordinated to zinc by the sulfonic acid group of the HEPES buffer used *in vitro* (35).

The EXAFS studies of zinc finger proteins, TFIIIA (33) and the glucocorticoid receptor (34), show clearly that there is not a unique environment for zinc in these systems (Fig. 4). Zinc bound to two histidine and two cysteine residues or four cysteinyl residues suggests that variants within the subset  $\text{Zn}(\text{histidine})_{4-x}(\text{cysteine})_x$  ( $x = 0-4$ ) should be considered. Also, the possibility implied by the GAL4 results, that the zinc sites may have some substitutional lability, raises further questions as to the role of zinc in the transcription of the genetic information stored in DNA.

## B. MERCURY

Nature has evolved a specific and ultrasensitive mercury(II) biosensor, MerR. This is a metalloregulatory protein and, as such, is a member of a class of metal-responsive factors that trigger cellular responses at the genetic level. MerR switches on the transcription of the bacterial mercuric ion resistance genes in the presence of nanomolar mercury(II). Mercury(II) binds stoichiometrically as one metal per MerR dimer, converting MerR from a repressor to a strong activator of transcription. Studies of site-specific mutations in each of the four cysteinyl residues per MerR monomer and UV-visible spectroscopic data clearly suggest the formation of Hg—S<sub>cys</sub> bonds. Mercury L<sub>III</sub>-EXAFS studies (38) have confirmed this and the data are consistent with a three-coordinate site with an average Hg—S distance of 2.43 Å. The coordination number is consistent with the bond length identified in  $[\text{Hg}(\text{SR})_3]^-$  complexes, whereas mononuclear  $[\text{Hg}(\text{SR})_2]$  and  $[\text{Hg}(\text{SR})_4]^{2-}$  complexes have Hg—S bonds of length 2.32–2.36 and 2.50–2.61 Å, respectively. Furthermore, chemical determinations show that three cysteinyl residues per dimer are protected by mercury(II) binding.

Bacterial mercuric reductase is a unique metal-detoxification biocatalyst, reducing mercury(II) salts to the metal. The enzyme contains flavin adenine dinucleotide, a reducible active site disulfide (Cys<sub>135</sub>, Cys<sub>140</sub>), and a C-terminal pair of cysteines (Cys<sub>558</sub>, Cys<sub>559</sub>). Mutagenesis studies have shown that all four cysteines are required for efficient mercury(II) reduction. Mercury L<sub>III</sub>-EXAFS studies for mercury(II) bound to both the wild-type enzyme and a very low-activity C-terminal double-alanine mutant (Cys<sub>135</sub>, Cys<sub>140</sub>, Ala<sub>558</sub>, Ala<sub>559</sub>) suggest the formation of an Hg(Cys)<sub>2</sub> complex in each case (39). The Hg—S distances obtained were 2.31 Å and are consistent with the correlation of bond length with coordination number presented above. Thus, no evidence was obtained for coordination of mercury(II) by all four active-site cysteines in the wild-type mercuric reductase. However, these studies do not define the full extent of the catalytic mechanism for mercury(II) reduction, and it is possible that a three- or four-coordinate Hg(Cys)<sub>n</sub> complex is a key intermediate in the process.

Mercury is known to substitute for copper in proteins, especially at “blue” copper sites because of the cysteinyl ligation (40). Such substitution may be helpful in selectively substituting copper sites in multicopper enzymes, such as laccase, thereby allowing the nature and function of the individual copper centers to be more clearly revealed.

Penner-Hahn and colleagues (41) have recorded the mercury L<sub>III</sub>-edge XAS for mercury-substituted plastocyanin, azurin, tree laccase, and stellacyanin. Analyses of the EXAFS data confirm that the mercury is selectively substituted at the “blue” (Type 1) copper-binding site in laccase and these data have provided the first direct structural information for this metal-binding site. In every case, the primary ligation of the mercury is achieved by two imidazole groups and one thiolate derived from the side chains of histidine and cysteine, respectively. Thus, the coordination geometry (but not the distances) is essentially the same, irrespective of whether copper or mercury is bound. As with copper K-edge EXAFS (42) it was not possible to identify the more weakly bonded ligands in the secondary coordination shell. However, the EXAFS and XANES data clearly point to these ligands being different in stellacyanin, as compared with the other three proteins.

The marked affinity of mercury for cysteinyl ligands, manifest in these XAS studies, points to a major biochemical perturbation upon incorporation of mercury(II) into a biological system, not least if substitution for copper occurs with a blocking of the activity of Type 1 sites. However, nature has also used this affinity for cysteinyl residues to bind mercury(II) for reduction and to switch on a process that pro-



vides cells with a mechanism to resist the invasion. This mechanism undoubtedly involves the synthesis of metallothionein.

### C. METALLOTHIONEINS

Metallothioneins are a unique and widely distributed group of proteins. They are characterized by their low molecular weight ( $\sim 6000$ ), high cysteinyl content, and the ability to bind substantial numbers of metal ions (43). The proteins bind copper and zinc, thereby providing a mobile pool as part of the normal metabolism of these elements, and offer protection from the invasion of inorganic forms of the toxic elements cadmium, lead, and mercury. In addition, other metals, such as iron and cobalt, can be induced to bind. XAS is ideally suited to probe the environment of these different metal atoms (see Fig. 1), and the structural interpretations obtained from an analysis of the EXAFS data obtained in several such studies are summarized in Table I (44). Thus, in each case, the data are consistent with the primary coordination of the metal deriving from the cysteinyl residues.

As indicated in Section II, uncertainties of  $\sim \pm 25\%$  in  $N$  are inherent in EXAFS from an analysis of the amplitude envelope alone. Therefore, appeal should be made to other information. For systems as simple as those in Table I, correlations of bond length with coordina-

TABLE I  
STRUCTURAL PARAMETERS DEDUCED FROM EXAFS  
OF METALLOTHIONEINS<sup>a</sup>

Absorber <sup>b</sup>	Scatterer	Radius (Å)
Zn in Zn <sub>7</sub> -MT	4S	2.33
Cu in Cu <sub>6</sub> Zn <sub>3</sub> -MT	3S	2.25
Cu in Cu <sub>5</sub> Zn <sub>2</sub> -MT	3S	2.25
Pb in Pb <sub>7</sub> -MT	2S	2.65
Hg in Hg <sub>7</sub> -MT	3S	2.42
Cd in Cd <sub>7</sub> -MT	4S	2.51
Cd in Cd <sub>4</sub> Co <sub>3</sub> -MT	4S	2.51
Co in Cd <sub>4</sub> Co <sub>3</sub> -MT	4S	2.30
Co in Co <sub>7</sub> -MT	4S	2.31
Co in Co <sub>3</sub> -MT	4S	2.31
Fe in Fe <sub>7</sub> -MT	4S	2.32
Fe in Fe <sub>3</sub> -MT	4S	2.32

<sup>a</sup> From Ref. 44.

<sup>b</sup> MT, Metallothionein.

tion number are helpful. Thus, for copper in pig liver metallothionein, reference may be made to crystallographic information for  $\text{Cu}(\text{SR})_2$ ,  $\text{Cu}(\text{SR})_3$ , and  $\text{Cu}(\text{SR})_4$  centers for which the Cu—S bond lengths are  $\sim 2.15$ ,  $2.24\text{--}2.29$ , and  $\sim 2.35$  Å, respectively. Thus, on this basis, copper would appear to be three-coordinate in the Cu,Zn-metallothioneins (31). Similarly, with reference to the Hg—SR bond length data presented in Section IV,C, mercury would also appear to be three-coordinate in Hg-metallothionein.

The first EXAFS studies of a cadmium environment in a protein were achieved for  $\text{Cd}_5\text{Zn}_2$ - and  $\text{Cd}_7$ -Metallothionein from rat liver (45). The two samples manifest identical EXAFS and the data are consistent with a shell of four sulfur atoms at  $\sim 2.51$  Å. These results demonstrate that the inequivalence of cadmium atoms observed by  $^{113}\text{Cd}$  NMR studies of metallothioneins (46) does not arise from marked variations in atom type, coordination number, or metal–ligand distances within the metals' first coordination sphere.

Clear evidence for the close approach of metal atoms in  $\text{Cd}_7$ -metallothionein is well established by  $^{113}\text{Cd}$  NMR spectroscopy. Indications of the intermetallic distances involved for cadmium and other metals have been sought from EXAFS. Although some indications of backscattering of metals bound within metallothioneins have been obtained (31, 47), the principal conclusion is that these metal–metal separations are not coherent. Therefore, the backscattered waves, especially with their high frequency at distances  $>3$  Å, engage in destructive interference, which effectively renders them "silent" in the EXAFS.

#### D. IRON STORAGE AND TRANSPORT PROTEINS

*Gold is for the mistress—silver for the maid—  
Copper for the craftsman cunning at his trade.  
"Good!" said the Baron, sitting in his hall,  
But Iron—Cold Iron—is master of them all.*

"Cold Iron"  
Rudyard Kipling

Iron can be said to be the most chemically versatile of all the elements used by nature. It is essential for dioxygen uptake and transport in the vast majority of living systems, is ubiquitous in electron transfer relays and oxygen metabolism, is used widely as the catalytic center in enzymes catalyzing chemical changes as diverse as dinitrogen fixation, nitrate reduction, and isopenicillin-*N*-synthase, and is vital for DNA

synthesis. However, the problem with storing large quantities of free iron in the body under physiological conditions is that soluble iron(III) ions react to form insoluble iron(III) oxide, the accumulation of which is toxic to cells. To avoid this, evolution has produced two iron storage proteins, ferritin and hemosiderin.

The major iron storage protein, ferritin, has been extensively studied (48) and shown to consist of a hollow, spherical proteinaceous shell surrounding an iron(III) oxide core. The other iron storage protein, hemosiderin, has received rather less attention, but, for "normal" hemosiderin, techniques such as  $^{57}\text{Fe}$  Mössbauer spectroscopy and electron diffraction (49) indicate the presence of a smaller ferritin-like core.

Iron K-edge XAS studies have been accomplished for ferritin (50, 51) and hemosiderin (51). These have allowed a direct comparison of structural aspects of the iron oxide cores of ferritin and hemosiderin, which could only be inferred from other techniques. The EXAFS recorded for horse spleen ferritin and "normal" hemosiderin are indistinguishable, consistent with them possessing an identical iron oxide core. The data are indicative of an average environment of the iron(III) consisting of six oxygen atoms at  $\sim 1.93$  Å and a split shell of iron atoms at  $\sim 2.95$  and  $\sim 3.38$  Å, together with a further oxygen shell at  $\sim 3.57$  Å (51). Iron K-edge EXAFS has been used to show that *Azotobacter vinelandii* ferritin and horse spleen ferritin can have essentially the same structure but that phosphate influences the local structure about iron. Thus, when the phosphate content is high, the iron atoms appear to possess five to six phosphorus neighbors at  $\sim 3.17$  Å. The incorporation of phosphate reduces the number of iron atoms present at  $\sim 3$  Å and increases the Fe—Fe separation to  $\sim 3.50$  Å. Therefore, some phosphates would appear to bridge neighboring iron atoms and act as chain termini as well (52).

The clinical condition thalassaemia, i.e., iron overload, results in serious tissue damage and eventual death. There are two stages in the progression of this disease, primary hemochromatosis and, the stage before death, secondary hemochromatosis. In both of these conditions, the predominant form of stored iron is hemosiderin, and not ferritin, as in healthy individuals. Iron K-edge XAS studies show that, for primary hemochromatosis, there is a dramatic change in the structure from "normal" hemosiderin. The EXAFS is a damped sinusoidal wave, representative of backscattering from a *single* shell of oxygen atoms at  $\sim 1.94$  Å. Therefore, the iron oxide core is amorphous. Secondary hemochromatosis hemosiderin reverts back to an ordered iron oxide core, with about three oxygens at  $\sim 1.90$  Å and three at  $\sim 2.03$  Å and a split

iron shell at  $\sim 2.97$  and  $\sim 3.34$  Å. Thus, there are also substantial structural differences between this and the iron oxide core of "normal" hemosiderin (51).

Iron is transported to and from the iron stores by transferrins. These proteins are single-chain polypeptides of  $\sim 80,000$  Da that are capable of binding two iron(III) atoms at specific binding sites. Protein crystallography and iron K-edge EXAFS data recorded for chicken ovotransferrin are consistent with the metal atoms possessing a first coordination shell of about six oxygen and/or nitrogen atoms, two at  $\sim 1.85$  Å and four at  $\sim 2.04$  Å. The shorter contact is suggested to arise from tyrosine ligation and the longer distance from histidine (N), bicarbonate, and water (O) ligation. Garratt *et al.* studied the C- and N-domain fragments separately and showed that the iron sites are not equivalent (53).

Phosvitins are a group of small phosphoglycoproteins that are the major components of the highly structured granules of the vertebrate egg yolk. These proteins have an unusually high ( $\sim 50\%$ ) serine content with extensive phosphorylation of these residues. Their biological role is not defined but it has been suggested that they participate in the transport of metals. Iron K-edge EXAFS data, recorded for the Fe-phosvitin from chicken eggs, show that the metal is bound to the protein in an octahedral environment. The principal binding is by the oxygen atoms of serine-bound phosphate groups at  $\sim 1.93$  Å from the metal (54).

#### E. ELECTRON TRANSFER CENTERS

The small protein rubredoxin ( $\sim 6000$  Da) possesses one iron atom tetrahedrally coordinated by four cysteinyl sulfur atoms. This center has been extensively studied by iron K-edge XAS (25, 55–57). Prior to these studies, the crystal structure of the iron(III) form of *Clostridium pasteurianum* rubredoxin had been determined by X-ray crystallography, suggesting that three of the Fe—S bonds were  $\sim 2.30$  Å and the fourth was  $\sim 2.05$  Å (average length  $2.24$  Å) (58). The advantages of combining EXAFS with protein crystallography were clearly demonstrated by these studies. Thus, the EXAFS data showed clearly that *all four* Fe—S bonds are of essentially the same length,  $\sim 2.26$  Å, in the oxidized protein. These studies led to a revision of the protein crystallographic conclusions (59) to be compatible with the EXAFS results. The latter were also able to identify an increase of  $\sim 0.06$  Å in Fe—S bond length upon reduction from iron(III) to iron(II), compatible with changes observed in a simple chemical analog (60). Although the original crystallographic results were cited as an example of the entatic

state (61), the general principle of that concept—that “the chemistry and energy of the protein fold generate an enforced stereochemistry and/or electronic state around a metal ion so as to enhance its potential catalytic function” (62)—remains unaltered by the bond length correction.

A situation similar to that outlined above for rubredoxin occurred for the 7Fe–7S ferredoxin of *A. vinelandii*. Thus spectroscopic studies, including iron K-edge EXAFS data for this and related systems (63, 64), caused crystallographers to reconsider and correct the structural details for the [3Fe–4S] center (65).

Type 1 (blue) copper sites are perhaps the best-characterized metalloprotein electron transfer centers. The molecular structures of four blue copper proteins—poplar plastocyanin (66), two azurins from *Pseudomonas aeruginosa* (67) and *Alcaligenes denitrificans* (68), and the “basic blue protein” from cucumbers (69)—are now known from protein crystallographic studies. In the copper(II) state of all four proteins, the primary coordination sphere of the metal consists of the nitrogen atoms of two histidine ligands and the sulfur atom of a cysteinyl residue. Copper K-edge EXAFS of both the oxidized and reduced states of Type 1 copper proteins (42, 70–73) detects these ligands clearly and at distances close to the crystallographic values (see also the review on blue copper proteins in this volume). These results are nicely summarized by Feiters *et al.* (73), and the data point to a modest ( $\leq 0.1$  Å) increase in the length of the metal–ligand bonds upon reduction.

Poplar plastocyanin involves the approach of the sulfur atom of a methionine residue at  $\sim 2.9$  Å to the copper (66). The significance of this ligand has attracted much discussion, with a much closer approach being detected in the reduced, protonated, form of the protein in which one histidine residue becomes detached from the copper(I) (74). EXAFS has been used to probe Type 1 copper centers, looking for differences in the secondary coordination to copper from protein to protein. However, backscattering from the methionine sulfur makes no significant contribution to the copper K-edge EXAFS, even at 4 K in frozen solution or at low ( $\sim 175$  K) temperature in single crystals oriented so that all of the Cu–S(Met) bonds were aligned parallel, and then perpendicular, to the polarization vector of the beam. The results provide a warning of the dangers of deriving structural results from poor EXAFS data. Furthermore, analysis of the near-edge structure gave direct evidence for X-ray-induced photoreduction of copper(II) plastocyanin when exposed to an extremely intense beam from a synchrotron (75).

## F. CENTERS INVOLVED IN OXYGEN METABOLISM

The photosynthetic water-splitting enzyme of chloroplasts is the source of dioxygen on this planet. The enzyme is located in the thylakoid membrane and, during turnover, it donates electrons to photosystem II and then oxidizes two molecules of  $\text{H}_2\text{O}$  to produce one molecule of  $\text{O}_2$ . Analytical and spectroscopic studies have demonstrated that a polynuclear manganese cluster is present at the heart of this enzyme.

XAS studies (76, 77) have progressed from manganese K-edge data to EXAFS of sufficient quality to give valuable structural information and allow direct comparisons with potential chemical analogs. The polarization inherent in synchrotron radiation has been used to good advantage to probe the manganese environment of the "resting" ( $\text{S}_1$ ) state of *oriented* spinach chloroplast membranes (77). These studies showed that the cluster is asymmetric and probably contains four manganese atoms with Mn—Mn distances of  $\sim 2.7$  and  $\sim 3.3$  Å, with the vector formed by the 3.3-Å pair being oriented perpendicular to the membrane plane. The manganese atoms are bonded to oxygen or nitrogen donor ligands at  $\sim 1.90$  and  $\sim 2.22$  Å, and it is expected that the manganese cluster is maintained by bridging ligands; the 2.7-Å separation is consistent with the presence of  $\mu_2$ -oxide or hydroxide groups and the 3.3-Å separation would be compatible with  $\mu_2$ -carboxylate ligation. Some of these conclusions contrast with those of Klein *et al.* (76), who investigated unorientated samples and obtained evidence for short ( $\sim 1.75$  Å) Mn—O/N interactions; these latter authors did, however, obtain evidence for the 2.7- and 3.3-Å Mn—Mn distances.

XAS has been used to probe each of the metal centers employed by nature to bind selectively dioxygen from air: hemoglobin, hemerythrin, and hemocyanin. With respect to hemoglobin, discussions have concentrated upon the Fe—N distances and the extent of the displacement of the iron atom out of the porphyrin plane upon deoxygenation. The crystal structure of deoxyhemoglobin has been refined (78) and gives essentially the same value for the distance of the iron to the porphyrin nitrogens as two independent iron K-edge EXAFS studies (79, 80), viz.  $\sim 2.06$  Å; this distance is some 0.08 Å longer than in oxyhemoglobin. Also, there is agreement that the displacement of the iron from the plane of the porphyrin nitrogens in deoxyhemoglobin is not as large as proposed ( $\sim 0.56$  Å) from earlier crystallographic studies (80); the distance to the proximal histidine nitrogen is  $\sim 2.12$  Å (81).

The XANES associated with the iron K-edge of hemoglobin (82) has been used to complement the EXAFS interpretations. XANES studies

have included myoglobin (83) and have addressed the geometry of its carbon monoxide complex (84). There are considerable attractions with respect to analyzing XANES data, not least being the prospect of obtaining angular, as well as radial, information. However, these attractions must not obscure the problems inherent to XANES, i.e., the limited data range, and the difficulty of establishing a unique interpretation together with an objective assessment of the precision of dimensions obtained (85).

Hemerythrin is a dioxygen-binding and transport protein found in several marine invertebrates. The active site of the protein involves two iron atoms, one of which binds a molecule of dioxygen but both of which are involved in the redox change attendant upon oxygenation; viz.  $2\text{Fe(II)} + \text{O}_2 \rightarrow 2\text{Fe(III)}(\text{O}_2^{2-})$ . The structure of hemerythrin has been determined by X-ray crystallography and the azido form has been shown to involve two hexacoordinate iron atoms linked by a  $\mu_2$ -oxo and two  $\mu_2$ -carboxylato ligands; both iron atoms are ligated to the protein by the imidazoles of histidinyll residues—one by three, and one by two, such groups—and the azide ion occupies the sixth coordination site of the second iron atom (86). Crystallographic studies of oxy- and deoxy-hemerythrin indicate that dioxygen binds in the same location as azide (87).

A careful iron K-edge XAS study has been accomplished for several forms of hemerythrin, including azido-, oxy-, and deoxyhemerythrin, and relevant well-defined chemical analogs have been used to calibrate the accuracy of data analysis. The most striking result obtained was that removal of dioxygen from oxyhemerythrin is accompanied by a decrease in the length of the  $\mu_2$ -O—Fe bond, from 1.82 to 1.98 Å; this change is held to be consistent with the corresponding conversion of a  $\mu_2$ -oxo group to a  $\mu_2$ -hydroxo group. The Fe—Fe distance expands proportionally, from 3.24 Å in oxyhemerythrin to 3.57 Å in deoxyhemerythrin, thus maintaining an approximately constant value for the Fe—O—Fe bridging angle. The length of the other bonds to the iron atoms, ~2.5 oxygens/nitrogens at ~2.12 and ~2.24 Å, change little upon deoxygenation (88).

The related binuclear iron sites in ribonucleotide reductase from *Escherichia coli* (89) and methane monooxygenase from *Methylococcus capsulatus* (Bath) (90) have also been characterized by iron K-edge XAS. For the former, one of the bonds to iron is considered to be a  $\mu_2$ -oxo group at 1.78 Å and the other atoms of the inner coordination sphere are oxygens (or nitrogens) at ~2.04 Å; the Fe—Fe distance is in the range 3.26–3.48 Å. For the latter, a  $\mu_2$ -hydroxo group is considered

to be present ( $\text{Fe—O} = 1.99 \text{ \AA}$ ), together with other oxygen (or nitrogen) atoms to give a first coordination shell of approximately six atoms at an average distance of  $\sim 2.05 \text{ \AA}$ ; the Fe—Fe separation is  $\sim 3.41 \text{ \AA}$ .

Hemocyanins are dioxygen-carrying proteins of mollusks and arthropods. They belong to the class of type 3 copper proteins and contain a binuclear site. The centers are colorless in their deoxy form and bind one molecule of dioxygen per center to generate a blue color; spectroscopic data are consistent with the redox change  $2\text{Cu(I)} + \text{O}_2 \rightarrow 2\text{Cu(II)(O}_2^{2-})$  on oxygenation. Protein crystallographic data for hemocyanin from the spiny lobster *Panulirus interruptus* has been reported (91) and copper K-edge data was used to establish that the crystals used for the X-ray determination contain virtually only deoxyhemocyanin (92). This study also showed that deoxy, oxy, and/or met [involving  $2\text{Cu(II)}$  atoms but no bound dioxygen] can coexist in the same crystal. This suggests that the conformations of the various forms are quite similar. Deoxyhemocyanin contains two copper atoms  $3.7 \text{ \AA}$  apart, each coordinated by three imidazole groups of histidine residues with no bridging ligand (91). Copper K-edge XAS studies of the oxy and deoxy forms of hemocyanin from a variety of sources were performed in advance of the crystallographic results (93–96). All EXAFS studies identify a Cu—Cu interaction at  $\sim 3.6 \text{ \AA}$  for oxyhemocyanins. The peroxide is a symmetrical bridging ligand, an oxygen atom of which is  $\sim 1.92 \text{ \AA}$  from each copper. Another light atom is considered to bridge the coppers, although the suggestion that this could derive from a tyrosinate residue is not compatible with the crystallographic data. In addition, each metal is considered to be ligated to two or three imidazole groups at  $\sim 2.0 \text{ \AA}$  (Fig. 5). However, in the EXAFS of deoxyhemocyanin, the Cu—Cu interaction is not clearly manifest. This “silence” may be a consequence of the lack of a bridging ligand that leads to uncorrelated motion of the copper atoms and a high Debye–Waller factor for the Cu—Cu “shell.” The Cu—N(His) distance becomes slightly smaller upon deoxygenation, consistent with the proposed reduction in coordination number (*vide ultra*) (see Fig. 5).

Superoxide dismutase catalyzes the disproportionation of superoxide as  $2\text{O}_2^- + 2\text{H}^+ \rightarrow \text{O}_2 + \text{H}_2\text{O}_2$ . The Cu,Zn-superoxide dismutases are widely distributed in both plant and animal kingdoms and are found in eukaryotic cytosols. The vast majority of studies on superoxide dismutases have been made on the enzyme from bovine erythrocytes; this enzyme contains 151 amino acid residues and two copper and two zinc atoms per molecule of  $\sim 32,000 \text{ Da}$ . The crystal structure of this protein has been reported (97), and the active site was shown to consist of a bimetallic (Cu,Zn) assembly (see Fig. 6). A type-2 copper center is



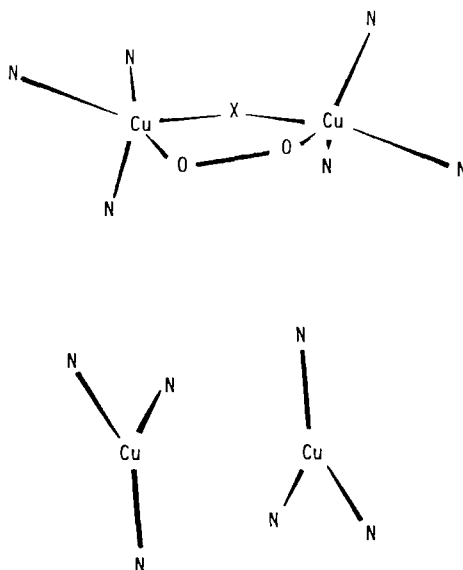


FIG. 5. Nature of the binuclear copper center in oxy- and deoxyhemocyanin proposed on the basis of copper K-edge EXAFS (93) (nitrogen atoms derive from imidazole groups of histidine residues; X is an oxygen or nitrogen atom).

identified, bound to four nitrogen atoms of one imidazolite and three imidazole groups of histidiny residues in a flattened tetrahedral arrangement. The imidazole group (*ex* histidine 61) bridges to zinc, which is also ligated by the nitrogen atoms of two imidazole groups of histidines and an oxygen atom of an aspartate carboxylate group.

Information obtained from the copper and zinc K-edge EXAFS (26), when set in the context of the crystallographic data, has improved the structural resolution of these metal sites and provided a clearer view of the involvement of these centers in the catalytic cycle (Fig. 6). The copper K-edge EXAFS for oxidized Cu,Zn-superoxide dismutase in solution shows clear evidence for the additional approach of a light atom—considered to be the oxygen of a kinetically labile water molecule (98)—at  $\sim 2.24$  Å from the copper(II). The accessibility of this site to anions has been confirmed by other XAS studies (99) and, thus, superoxide is expected to bind at copper(II) also. Reduction of the enzyme produces copper(I) and results in a significant change in the geometry of the site. Specifically, the Cu–N(His) distances shorten from  $\sim 1.99$  to  $\sim 1.94$  Å and the EXAFS amplitude suggests the presence of three rather than four coordinated imidazoles. The nature of the bond length change is indicative of a coordination number of cop-

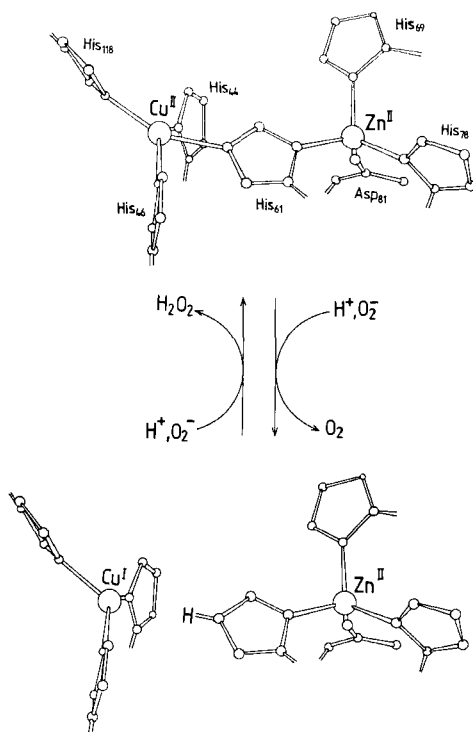


FIG. 6. Mechanism proposed for the disproportionation of superoxide by Cu, Zn-superoxide dismutase.

per, which is lower in the reduced than in the oxidized enzyme, because simple reduction of copper(II) to copper(I) is expected to *lengthen* the bonds.

EXAFS cannot identify which imidazole group is removed from the copper upon reduction. This process has been shown to be coupled to a protonation of the bridging imidazolate on the copper side (100); therefore, the cleavage of the bridging residue (His 61) from copper might be anticipated. Several  $^1\text{H}$  NMR spectroscopic studies have addressed this problem and various possibilities have been suggested; the latest work favors the detachment of His 61 upon reduction (101).

Examination of the XAS data recorded at the zinc K-edge indicates that the stereochemistry at zinc is essentially unperturbed by reduction at copper. Thus, the zinc(II) center is considered to play a structural role, holding the protonated imidazole group adjacent to the copper(I) center, to enable the second stage of the disproportionation to proceed by the protonation and reduction of superoxide (Fig. 6).

Laccase contains four copper atoms and catalyzes the four-electron reduction of dioxygen to water. X-Ray absorption edge spectroscopy has been used to determine the oxidation states of copper in *Rhus vernicifera* laccase, following the reaction of the reduced enzyme with dioxygen (102). This study included the incorporation of mercury(II) in the Type 1 copper site (see Section IV,B). The results demonstrate that the Type 2/Type 3 trinuclear copper site, as found in ascorbate oxidase (103), represents the minimal active site required for the multielectron reduction of dioxygen.

### G. OXOMOLYBDOENZYMES

Molybdenum is the most important 4d transition metal within the biosphere and is essential for the activity of a large group of enzymes (104). For many of these, clear evidence has been obtained that molybdenum is the site of substrate binding and conversion. These enzymes are found in organisms that range from bacteria to man; in the former, molybdenum is involved in nitrogen fixation and in the latter it is involved in xanthine and sulfite oxidation. There is a clear biochemical distinction between the nitrogenases on the one hand and oxomolybdoenzymes—such as xanthine oxidase and dehydrogenase, sulfite and aldehyde oxidase, and nitrate reductase—on the other. Such a distinction was initially apparent from EPR spectroscopy (105) and was subsequently reinforced by the isolation of the iron–molybdenum cofactor (FeMoco) from the nitrogenases (106) and the molybdopterin cofactor (Moco) from the oxomolybdoenzymes (107, 108).

XAS has played a vital role in defining the chemical nature of these molybdenum centers and how they respond to changes in the oxidation level of the protein and/or to the presence of substrates, substrate analogs, or inhibitors of enzymatic activity (9, 13, 15). The prefix *oxo* for this latter group of enzymes is appropriate. Thus, not only does each enzyme catalyze a conversion, the net result of which can be represented as oxygen atom transfer, but also XAS studies have confirmed the presence of at least one terminal oxo ligand ( $\text{Mo}=\text{O}$ ) for molybdenum in each of the enzymes.

Sulfite oxidase is responsible for the physiological oxidation of sulfite to sulfate. The molybdenum K-edge EXAFS results achieved (109) for this enzyme are the clearest such data and the interpretation achieved represents a prototype for other oxomolybdoenzymes. The molybdenum site has been investigated in each of its three accessible oxidation states [(VI), (V), and (IV)] as a function of pH and chloride concentration. The molybdenum(VI) is coordinated to two oxo groups,

at  $\sim 1.70$  Å, one oxygen-donor (or nitrogen-donor) and three sulfur-donor ligands at  $\sim 2.06$  and  $\sim 2.42$  Å, respectively. Two of these sulfur atoms would be expected to arise from the molybdopterin (108). The molybdenum(VI) center is not affected by changing the pH from 6 to 9 or by a variation in the chloride concentration.

The reduced molybdenum centers each possess a single oxo ligand, at  $\sim 1.69$  Å, one oxygen-donor (or nitrogen-donor) and three sulfur-donor ligands at  $\sim 2.00$  and  $\sim 2.37$  Å, respectively. Both of these centers appear to bind a chloride ligand at pH 6 in 0.3 M KCl. The results for molybdenum(V) have a special significance, in that they permit a direct comparison of the EXAFS results with EPR data. EPR spectroscopy (105) shows that the center can exist in two different forms, which are in a pH- and anion-dependent equilibrium. George *et al.* (109) concluded that the molybdenum K-edge EXAFS data were consistent with one chloride ligand binding to the low-pH form and that the number of oxo groups remains the same upon transition from the high-pH to the low-pH molybdenum(V) form.

Thus, for sulfite oxidase, a clear picture emerges from the interpretation of the EXAFS data. Reduction of molybdenum(VI) results in the loss of one oxo group, presumably due to protonation, and the generation of an anion-binding site. The behavior is consistent with the chemistry of molybdenum in its higher oxidation states. A *cis*-dioxomolybdenum(VI) center is generally converted to a monooxomolybdenum(V) or (IV) center upon reduction, provided that steric restrictions prevent dimerization—as would be expected for the molybdenum centers in enzymes. These changes are crucial for the mediation of oxygen atom transfer, which is formally a two-electron process and is difficult to accomplish, except by atom transfer.

Xanthine oxidase is the most available of the oxomolybdoenzymes and is readily extracted from cow's milk. This enzyme exists in two forms: active and an inactive form caused by loss of a sulfur atom (desulfo). Molybdenum K-edge EXAFS studies (110) have shown that the environments of molybdenum(VI) and molybdenum(IV) in desulfo xanthine oxidase closely resemble that of the corresponding oxidation state for sulfite oxidase. The principal difference between the center of the oxidized active form, as compared to the oxidized desulfo form, is the presence of one sulfido group (at  $\sim 2.18$  Å) plus one oxo group, rather than two oxo groups. The molybdenum center of xanthine oxidase is very reactive and both molybdenum K-edge EXAFS and EPR data indicate that the center of this reactivity is the Mo=S bond. The terminal sulfido group is lost upon reduction, presumably protonated to form an Mo-SH moiety. Arsenite is a potent inhibitor of xanthine

oxidase and the nature of the species formed has been probed by EXAFS at both the molybdenum and arsenic K-edges. Clear evidence for an Mo—S—As interaction, with an interbond angle of  $\sim 80^\circ$ , was obtained (111).

Alloxanthine forms a tight complex with the molybdenum(IV) center of xanthine oxidase. This complex is of clinical importance because it is the inhibitory product of xanthine oxidase with allopurinol used in the treatment of hyperuricemia. The molybdenum K-edge EXAFS of this complex is consistent with the structure shown in Fig. 7. Similarly, the molybdenum(IV) complex, formed when violapterin reacts with the enzyme, has lost the short Mo=S bond (112). Oxidation of the alloxanthine complex (Fig. 7) produces a molybdenum(V) center. This species manifests an EPR spectrum closely resembling that of the "very rapid" signal of a transient considered to be of catalytic significance in the oxidation of xanthine (105). This EPR spectrum exhibits unusually large  $^{33}\text{S}$  hyperfine coupling and a lack of proton hyperfine coupling, consistent with the conversion of the Mo—SH (Fig. 7) to Mo=S (113).

Nitrate is the major source of nitrogen for most green plants and fungi and may also be used by microorganisms as the terminal electron acceptor in place of dioxygen for anaerobic metabolism. The enzymes responsible for the first step in nitrate assimilation and for nitrate respiration are the nitrate reductases. These are oxomolybdoenzymes that catalyze the reduction of nitrate to nitrite. Molybdenum K-edge EXAFS studies have been reported for the assimilatory enzyme of *Chlorella vulgaris* and the dissimilatory enzyme of *E. coli* (114, 115). The former is a homotetramer of  $\sim 360,000$  Da that contains one molybdenum, one heme, and one FAD per subunit, and the latter is a heterodimer of  $\sim 200,000$  Da containing one molybdenum, 4[4Fe—4S], and a cytochrome *b* unit. The molybdenum environment of the *Chlorella* enzyme strongly resembles that in sulfite oxidase. In the oxidized state, the molybdenum is bound to two terminal oxygens at  $\sim 1.71$  Å

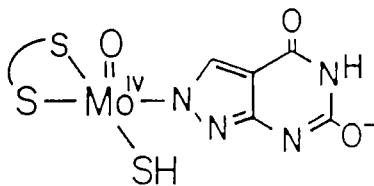


FIG. 7. Structure of the complex formed between alloxanthine and the molybdenum(IV) center of xanthine oxidase consistent with EXAFS and EPR results ( $\widehat{\text{S}}\text{—S}$  = pterin ligation) (110, 111).

plus about three sulfurs at  $\sim 2.44$  Å. A single terminal oxygen at  $\sim 1.67$  Å and a set of about three sulfurs at  $\sim 2.37$  Å are present in the reduced [molybdenum(IV)] form.

The original EXAFS studies of the *E. coli* enzyme (114) were accomplished before anion binding to the enzyme was known to occur and under conditions that made comparisons with EPR data difficult. A reexamination of these EXAFS data (115) addressed both of these important aspects. The fully oxidized [molybdenum(VI)] and fully reduced [molybdenum(IV)] species were characterized and the EPR signals of the small amount of the residual [molybdenum(V)] were used as an indication of sample homogeneity. However, possible deficiencies in this approach need to be noted and these may be relevant to the difficulties encountered in data analysis, notably the observation of non-stoichiometric amounts of Mo=O species. The molybdenum environment in the oxidized form of *E. coli* nitrate reductase at pH 6.8 resembles that of the corresponding form of sulfite oxidase. However, only one oxo group appears to be present. Also, a pH- and anion-dependent equilibrium occurs for this (oxidized) state with the anion (chloride) being bound at low pH (6.8) and lost at high pH (10.2). Reduction to molybdenum(IV) leads to a significant reduction in the backscattering contribution from the Mo=O groups, with a pH- and anion-dependent equilibrium similar to the oxidized form being observed.

A striking feature of these EXAFS studies is the observation that a substantial proportion of the molecules of *E. coli* nitrate reductase—in the reduced form at pH 6.8 and the oxidized and reduced forms at pH 10.2—appear to lack oxo groups. Such systems appear to be unique among the “oxo” molybdoenzymes.

## H. NITROGENASES

Nitrogen is an essential element for life and is abundant in the Earth's atmosphere in the form of molecular dinitrogen. Dinitrogen is, however, not metabolized by most organisms. Consequently, they must obtain their nitrogen in a chemically combined form, e.g., as ammonia, nitrate, or an organic molecule. Because organic nitrogen is incompletely recycled in living ecosystems and the available ammonia and nitrate are continually metabolized to dinitrogen through nitrification and denitrification, all life ultimately depends upon the biological fixation of dinitrogen.

Nitrogen fixation occurs only in certain prokaryotes and is catalyzed by the nitrogenases, which have two protein components. These are the Fe-protein, which acts as a specific reductant of the larger MoFe-

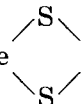
protein. Within the latter there are at least six metal-containing prosthetic groups, including two iron-molybdenum cofactors (FeMoco), which are the catalytic centers of the enzyme (see Eady, this volume).

One of the earliest successful applications of EXAFS to probe a metalloenzyme was the study of the molybdenum site of nitrogenase. Studies were made on both the *C. pasteurianum* and *A. vinelandii* MoFe-proteins and on isolated FeMoco (116). These studies showed definitively that molybdenum is present as part of a polynuclear cluster containing sulfur and iron, with Mo—S and Mo—Fe distances of  $\sim 2.36$  and  $\sim 2.72$  Å, respectively. This work inspired the successful development of many chemical systems containing Mo—Fe—S clusters, and XAS studies of these systems strengthened the basis for the interpretation of corresponding data for the natural system. The most accurate picture of the molybdenum site of FeMoco currently available involves a coordination of about three oxygen (or nitrogen), sulfur, and iron atoms at  $\sim 2.10$ ,  $\sim 2.37$ , and  $\sim 2.70$  Å, respectively (117).

Genetic suppression of the "normal" molybdenum-dependent nitrogenase of certain classes of *Azotobacter* allows expression of the vanadium-dependent enzyme. The vanadium and molybdenum nitrogenase systems show many similarities, and, in particular, an iron-vanadium cofactor (FeVaco), analogous to FeMoco, has been isolated (118). Clear evidence of a strong similarity between active sites in the MoFe- and VFe-proteins has been provided by vanadium K-edge XAS studies. Two VFe-proteins have been investigated, one from *Azotobacter chroococcum* (119, 120) and one from *A. vinelandii* (121). The edge structure shows a weak, single  $1s \rightarrow 3d$  transition, the intensity of which precludes the presence of terminal V=O bonds and implies an octahedral coordination around vanadium. The edge and XANES structure is very similar to that recorded for a  $VFe_3S_4$  cubanelike cluster  $[NMe_4][VFe_3S_4Cl_3(DMF)_3]$  (122). The EXAFS results (119, 120) are consistent with vanadium in the VFe-protein of *A. chroococcum* being ligated by about three oxygen (or nitrogen), sulfur, and iron atoms at  $\sim 2.13$ ,  $\sim 2.33$ , and  $\sim 2.75$  Å, respectively. The vanadium would thus appear to substitute for molybdenum in FeMoco to form FeVaco. The role of these metals has still to be elucidated. Possibly they facilitate redox reactions within the cluster and, therefore, it is noteworthy that neither the molybdenum nor the vanadium center experiences any significant structural change as the oxidation level of the cofactor is varied.

The average environment of iron in FeMoco (see Fig. 2) (19) and FeVaco (123) has been investigated by XAS. These data provide clear evidence for the two cofactors possessing the same molecular topology

and give further insights into their internal organization. Specifically, a longer range structural order is identified at  $\sim 3.68$  Å (see the Fourier transform of Fig. 2) corresponding primarily to Fe—Fe back-scattering. This situation is in clear contrast to that for the metallothioneins (Section IV,C) and indicates that these longer Fe—Fe distances are *coherent*. Furthermore, the iron atoms are ligated essentially by sulfurs at  $\sim 2.20$  Å and the cofactors are primarily com-

posed of Fe  Fe(M) (M=Mo,V) rhombs with metal-metal separations of 2.65–2.75 Å.

#### ACKNOWLEDGMENTS

In this review there has been an attempt to present a balanced view of the contributions made by X-ray absorption spectroscopy to the characterization of transition metal centers in proteins. No attempt has been made to be comprehensive and apologies are due to those whose work has been omitted, often on a quite arbitrary basis.

The author's involvement with X-ray absorption spectroscopy has been made enjoyable and scientifically stimulating by the ability, commitment, and good humor of many colleagues and collaborators to whom the credit belongs for any achievements. A particular debt is owed to Dr. S. S. Hasnain and Dr. G. P. Diakun of The Daresbury Laboratory; to the research students Ian Ross, Ian Abrahams, Eileen Wardell, Annette Flood, John Baines, Bryan Edwards, and Tricia Mackle; and to postdoctoral research assistants Norman Binsted, Judith Arber, John Charnock, and Ian Harvey. The Director and the staff at The Daresbury Laboratory are thanked for the provision of the facilities necessary to accomplish the research and the Science and Engineering Council are acknowledged for the provision of financial support. I am also greatly indebted to Mrs. Christine Metcalfe for her diligence and patience during the preparation of this manuscript.

#### REFERENCES

1. Williams, R. J. P., *Biol. Rev. Cambridge Philos. Soc.* **28**, 381 (1953).
2. Williams, R. J. P., *Q. Rev., Chem. Soc.* **24**, 331 (1970).
3. Williams, R. J. P., *Eur. J. Biochem.* **150**, 231 (1985).
4. Williams, R. J. P., *Coord. Chem. Rev.* **100**, 573 (1990).
5. Kincaid, B. M., and Eisenberger, P., *Phys. Rev. Lett.* **34**, 1361 (1975).
6. Cramer, S. P., and Hodgson, K. O., *Prog. Inorg. Chem.* **25**, 1 (1979).
7. Lee, P. A., Citrin, P. H., Eisenberger, P., and Kincaid, B. M., *Rev. Mod. Phys.* **53**, 769 (1981).
8. Powers, L., *Biochim. Biophys. Acta* **683**, 1 (1982).
9. Cramer, S. P., *Adv. Inorg. Bioinorg. Mech.* **2**, 259 (1983).



10. Scott, R. A., in "Methods in Enzymology" (C. H. W. Hirs and S. N. Timasheff, eds.), Vol. 117, p. 414. Academic Press, Orlando, Florida, 1985.
11. Hasnain, S. S., *Life Chem. Rep.* **4**, 273 (1987).
12. Hasnain, S. S., and Garner, C. D., *Prog. Biophys. Mol. Biol.* **50**, 47 (1987).
13. Cramer, S. P., in "X-ray Absorption Spectroscopy" (D. C. Koningsberger and R. Prins, eds.), p. 257. Wiley, New York, 1988.
14. Labhardt, A., and Yuen, C., *Nature (London)* **277**, 150 (1979).
15. Hedman, B., Hodgson, K. O., and Garner, C. D., in "Synchrotron Radiation and Biophysics" (S. S. Hasnain, ed.), p. 43. Ellis Horwood, Chichester, 1990.
16. Lee, P. A., and Pendry, J. B., *Phys. Rev. B: Solid State* [3] **11**, 2795 (1975).
17. Ashley, C. A., and Doniach, S., *Phys. Rev. B: Solid State* [3] **11**, 1279 (1975).
18. Gurman, S. J., Binsted, N., and Ross, I., *J. Phys. C* **17**, 143 (1984).
19. Arber, J. M., Flood, A. C., Garner, C. D., Gormal, C. A., Hasnain, S. S., and Smith, B. E., *Biochem. J.* **252**, 421 (1988).
20. Sayers, D. E., Stern, E. A., and Lytle, F. W., *Phys. Rev. Lett.* **27**, 1204 (1971).
21. Joyner, R. W., Martin, K. J., and Meeham, P., *J. Phys. C* **20**, 4005 (1987).
22. Gurman, S. J., Binsted, N., and Ross, I., *J. Phys. C* **19**, 1845 (1986).
23. Strange, R. W., Blackburn, N. J., Knowles, P. F., and Hasnain, S. S., *J. Am. Chem. Soc.* **109**, 7157 (1987).
24. Durham, P. J., Pendry, J. B., and Hodges, C. H., *Comput. Phys. Commun.* **25**, 193 (1982).
25. Shulman, R. G., Eisenberger, P., Teo, B.-K., Kincaid, B. M., and Brown, G. S., *J. Mol. Biol.* **124**, 305 (1978).
26. Blackburn, N. J., Hasnain, S. S., Binsted, N., Diakun, G. P., Garner, C. D., and Knowles, P. F., *Biochem. J.* **219**, 985 (1984).
27. Williams, R. J. P., *Endeavour [N.S.]* **8**, 65 (1984).
28. Vallee, B. L., *Met. Ions Biol.* **5**, 1 (1983).
29. Colman, P. M., Jansonius, J. N., and Matthews, B. W., *J. Mol. Biol.* **70**, 101 (1972); Richardson, J. S., Thomas, K. A., Rubin, B. H., and Richardson, D. C., *Proc. Natl. Acad. Sci. U.S.A.* **76**, 1349 (1979); Rees, D. C., Lewis, M., Konzato, R. B., Lipscomb, W. N., and Hardman, K. D., *ibid.* **78**, 3408 (1981).
30. Garner, C. D., and Feiters, M., in "Biophysics and Synchrotron Radiation" (A. Bianconi and A. Congiu-Castellano, eds.), p. 136. Springer-Verlag, Berlin, 1987.
31. Abrahams, I. L., Garner, C. D., Bremner, I., Diakun, G. P., and Hasnain, S. S., *Biochem. J.* **236**, 585 (1986).
32. Phillips, J. C., Bordas, J., Foote, A. M., Koch, M. J. H., and Moody, M. F., *Biochemistry* **21**, 830 (1982).
33. Diakun, G. P., Fairall, L., and Klug, A., *Nature (London)* **324**, 698 (1986).
34. Freedman, L. P., Luisi, B. F., Korszun, Z. R., Basavappa, R., Sigler, P. B., and Yamamota, K. R., *Nature (London)* **334**, 541 (1988).
35. Povey, J. F., Diakun, G. P., Garner, C. D., Wilson, S. P., and Laue, E. D., *FEBS Lett.* **266**, 142 (1990).
36. Pan, T., and Coleman, J. E., *Proc. Natl. Acad. Sci. U.S.A.* **86**, 3145 (1989).
37. Swenson, D., Baenzinger, N. C., and Coucouvanis, D., *J. Am. Chem. Soc.* **100**, 1932 (1978).
38. Wright, J. G., Tsang, H.-T., Penner-Hahn, J. E., and O'Halloran, T. V., *J. Am. Chem. Soc.* **112**, 2434 (1990).
39. Raybuck, S. A., Distefano, M. D., Teo, B.-K., Orme-Johnson, W., and Walsh, C. T., *J. Am. Chem. Soc.* **112**, 1983 (1990).
40. Church, W. B., Guss, J. M., Potter, J. J., and Freeman, H. C., *J. Biol. Chem.* **261**, 234 (1986).

41. Klemens, A. S., McMillin, D. R., Tsang, H.-T., and Penner-Hahn, J. E., *J. Am. Chem. Soc.* **111**, 6398 (1989).
42. Scott, R. A., Hahn, J. E., Doniach, S., Freeman, H. C., and Hodgson, K. O., *J. Am. Chem. Soc.* **104**, 5364 (1982).
43. Vasak, M., and Kagi, J. H. R., *Met. Ions Biol. Syst.* **15**, 213 (1988).
44. Charnock, J. M., Garner, C. D., Abrahams, I. L., Arber, J. M., Hasnain, S. S., Henahan, C., and Vasak, M., *Physica B (Amsterdam)* **158**, 93 (1989).
45. Abrahams, I. L., Garner, C. D., Bremner, I., Diakun, G. P., and Hasnain, S. S., *J. Am. Chem. Soc.* **107**, 4596 (1985).
46. Otvos, J. D., and Armitage, I., *Proc. Natl. Acad. Sci. U.S.A.* **77**, 7904 (1980).
47. Freeman, J. H., Powers, L., and Peisach, J., *Biochemistry* **25**, 2342 (1986).
48. Ford, G. C., Harrison, P. M., Rice, D. W., Smith, J. M. A., Treffry, A., White, J. L., and Yariv, J., *Philos. Trans. R. Soc. London, Ser. B* **1984**, **304**, 551 (1984); Harrison, P. M., Andrews, S. C., Ford, G. C., Smith, J. M. A., Treffry, A., and White, J. L., in "Iron Transport in Microbes, Plants, and Animals" (G. Winkelmann, D. Van der Helm, and J. B. Neilands, eds.), p. 445. VCH Publ., New York, 1987.
49. Bell, S. H., Weir, M. P., Dickson, D. P. E., Gibson, J. F., Sharp, G. A., and Peters, T. J., *Biochim. Biophys. Acta* **787**, 227 (1984); Dickson, D. P. E., Reid, N. M. K., Mann, S., Wade, V. J., Ward, R. J., and Peters, T. J., *ibid.* **957**, 81 (1988).
50. Islam, Q. T., Sayers, D. E., Gorum, S. M., and Theil, E. C., *J. Inorg. Biochem.* **36**, 51 (1989); Theil, E. C., Sayers, D. E., and Brown, M. A., *J. Biol. Chem.* **254**, 8132 (1979); Heald, S. M., Stern, E. A., Bunker, B., Holt, E. M., and Holt, S. L., *J. Am. Chem. Soc.* **101**, 67 (1979).
51. Mackle, P., Garner, C. D., Ward, R. J., and Peters, T. J., submitted.
52. Rohrer, J. S., Islam, Q. T., Watt, G. D., Sayers, D. E., and Theil, E. C., *Biochemistry* **29**, 259 (1990).
53. Garratt, R. C., Evans, R. W., Hasnain, S. S., and Lindley, P. F., *Biochem. J.* **233**, 479 (1986).
54. Mangani, S., Orioli, P., Scozzafava, A., Messori, L., and Stern, E. A., *Inorg. Chem.* **29**, 124 (1990).
55. Shulman, R. G., Eisenberger, P., Blumberg, W. E., and Stombaugh, N. A., *Proc. Natl. Acad. Sci. U.S.A.* **72**, 4003 (1975).
56. Citrin, P. H., Eisenberger, P., and Kincaid, B. M., *Phys. Rev. Lett.* **36**, 1346 (1976).
57. Sayers, D. E., Stern, E. A., and Herriott, J. R., *J. Chem. Phys.* **64**, 427 (1976).
58. Watenpaugh, K. D., Sieker, L. C., Herriott, J. R., and Jensen, L. H., *Acta Crystallogr.* **29**, 943 (1973).
59. Watenpaugh, K. D., Sieker, L. C., and Jensen, L. H., *J. Mol. Biol.* **138**, 615 (1980).
60. Lane, R. W., Ibers, J. A., Frankel, R. B., Papaefthymiou, G. C., and Holm, R. H., *J. Am. Chem. Soc.* **99**, 84 (1977).
61. Vallee, B. L., and Williams, R. J. P., *Proc. Natl. Acad. Sci. U.S.A.* **59**, 498 (1968).
62. Williams, R. J. P., *J. Mol. Catal.* **30**, 1 (1985).
63. Stephens, P. J., Morgan, T. V., Devlin, F., Penner-Hahn, J. E., Hodgson, K. O., Scott, R. A., Stout, C. D., and Burgess, B. K., *Proc. Natl. Acad. Sci. U.S.A.* **82**, 5661 (1985).
64. Antonio, M. R., Averill, B. A., Moura, I., Moura, J. J. G., Orme-Johnson, W. H., Teo, B.-K., and Xavier, A. V., *J. Biol. Chem.* **257**, 6646 (1982).
65. Stout, G. H., Turley, S., Sieker, L. C., and Jensen, L. H., *Proc. Natl. Acad. Sci. U.S.A.* **85**, 1020 (1988); Stout, C. D., *J. Biol. Chem.* **263**, 9256 (1988).
66. Colman, P. M., Freeman, H. C., Guss, J. M., Murata, M., Norris, V. A., Ramshaw,

- J. A. M., and Venkatappa, M. P., *Nature (London)* **272**, 319 (1978); Guss, J. M., and Freeman, H. C., *J. Mol. Biol.* **169**, 521 (1983).
67. Adman, E. T., Stenkamp, R. E., Sieker, L. C., and Jensen, L. H., *J. Mol. Biol.* **123**, 35 (1978); Adman, E. T., and Jensen, L. H., *Isr. J. Chem.* **21**, 8 (1981).
68. Norris, G. E., Anderson, B. F., and Baker, E. N., *J. Am. Chem. Soc.* **108**, 2784 (1986).
69. Guss, J. M., Merritt, E. A., Phizackerley, R. P., Hedman, B., Murata, M., Hodgson, K. O., and Freeman, H. C., *Science* **241**, 806 (1988).
70. Tullius, T. D., Frank, P., and Hodgson, K. O., *Proc. Natl. Acad. Sci. U.S.A.* **75**, 4069 (1978).
71. Peisach, J., Powers, L., Blumberg, W. E., and Chance, B., *J. Biophys. Soc.* **38**, 277 (1982).
72. Groenvelde, C. M., Feiters, M. C., Hasnain, S. S., van Rijn, J., Reedijk, J., and Canters, G. W., *Biochim. Biophys. Acta* **873**, 214 (1986).
73. Feiters, M. C., Dahlin, S., and Reinhammar, B., *Biochim. Biophys. Acta* **955**, 250, and references therein (1988).
74. Guss, J. M., Harrowell, P. R., Murata, M., Norris, V. A., and Freeman, H. C., *J. Mol. Biol.* **192**, 361 (1986).
75. Penner-Hahn, J. E., Murata, M., Hodgson, K. O., and Freeman, H. C., *Inorg. Chem.* **28**, 1826 (1989).
76. Kirby, J. A., Goodin, D. B., Wydrzynski, T., Robertson, A. S., and Klein, M. P., *J. Am. Chem. Soc.* **103**, 5537 (1981); Yachandra, V. K., Guiles, R. D., McDermott, A. E., Britt, R. D., Dexheimer, S. L., Sauer, K., and Klein, M. P., *Biochim. Biophys. Acta* **850**, 324 (1986); Yachandra, V. K., Guiles, R. D., McDermott, A. E., Cole, J. L., Britt, R. D., Dexheimer, S. L., Sauer, K., and Klein, M. P., *Biochemistry* **26**, 2974 (1987).
77. George, G. N., Prince, R. C., and Cramer, S. P., *Science* **243**, 789 (1989).
78. Fermi, G., Perutz, M. F., and Shulman, R. G., *Proc. Natl. Acad. Sci. U.S.A.* **84**, 6167 (1987).
79. Eisenberger, P., Shulman, R. G., Kincaid, B. M., Brown, G. S., and Ogawa, S., *Nature (London)* **274**, 30 (1978).
80. Perutz, M. F., Hasnain, S. S., Duke, P. J., Sessler, J. L., and Hahn, J. E., *Nature (London)* **295**, 535 (1982).
81. Perutz, M. F., *Nature (London)* **228**, 726 (1970).
82. Congui-Castellano, A., Castagnola, M., Burattini, E., Dell'Ariceia, M., Longa, S. D., Giovannelli, A., Durham, P. J., and Bianconi, A., *Biochim. Biophys. Acta* **996**, 240 (1989).
83. Shiro, Y., Sato, F., Suzuki, T., Iizuka, T., Matsushita, T., and Oyanagi, H., *J. Am. Chem. Soc.* **112**, 2921 (1990).
84. Bianconi, A., Congui-Castellano, A., Durham, P. J., Hasnain, S. S., and Phillips, S. E. V., *Nature (London)* **318**, 765 (1985).
85. Galloway, J., *Nature (London)* **318**, 602 (1985).
86. Stenkamp, R. E., Sieker, L. C., and Jensen, L. H., *J. Am. Chem. Soc.* **106**, 618 (1984).
87. Stenkamp, R. E., Sieker, L. C., Jensen, L. H., McCallum, J., and Sanders-Loehr, J., *Proc. Natl. Acad. Sci. U.S.A.* **82**, 713 (1985).
88. Zhang, K., Stern, E. A., Ellis, F., Sanders-Loehr, J., and Shiemke, A. K., *Biochemistry* **27**, 7470 (1988).
89. Bunker, G., Petersson, L., Sjöberg, B.-M., Sahlin, M., Chance, M., Chance, B., and Ehrenberg, A., *Biochemistry* **26**, 4708 (1987).

90. Ericson, A., Hedman, B., Hodgson, K. O., Green, J., Dalton, H., Bentson, J. G., Beer, R. H., and Lippard, S. J., *J. Am. Chem. Soc.* **110**, 2330 (1988).
91. Gaykema, W. P. J., Hol, W. G. J., Vereijken, J. M., Soeter, N. M., Bak, H. J., and Beintema, J. J., *Nature (London)* **309**, 23 (1984); Gaykema, W. P. J., Volbeda, A., and Hol, W. G. J., *J. Mol. Biol.* **187**, 255 (1985).
92. Volbeda, A., Feiters, M. C., Vincent, M. G., Bouwman, E., Dobson, B., Kalk, K. H., Reedijk, J., and Hol, W. G. J., *Eur. J. Biochem.* **181**, 669 (1989).
93. Brown, J. M., Powers, L., Kincaid, B., Larrabee, J. A., and Spiro, T. G., *J. Am. Chem. Soc.* **102**, 4210 (1980).
94. Co, M.-S., Hodgson, K. O., Eccles, T. K., and Lontie, R., *J. Am. Chem. Soc.* **103**, 984 (1981).
95. Co, M.-S., and Hodgson, K. O., *J. Am. Chem. Soc.*, **103**, 3200 (1981).
96. Woolery, G. L., Powers, L., Winkler, M., Solomon, E. I., and Spiro, T. G., *J. Am. Chem. Soc.* **106**, 86 (1984).
97. Tainer, J. A., Getzoff, E. D., Beem, K. M., Richardson, J. S., and Richardson, D. C., *J. Mol. Biol.* **160**, 181 (1982).
98. Fee, J. A., and Gaber, B. P., *J. Biol. Chem.* **247**, 60 (1972); Boden, N., Holmes, M. C., and Knowles, P. F., *Biochem. J.* **177**, 303 (1979).
99. Blackburn, N. J., Strange, R. W., McFadden, L. M., and Hasnain, S. S., *J. Am. Chem. Soc.* **109**, 7162 (1987).
100. McAdam, M. E., Fielden, E. M., Lavelle, F., Calabrese, L., Cocco, D., and Rotilio, G., *Biochem. J.* **167**, 271 (1977).
101. Paci, M., Desideri, A., Sette, M., Ciriolo, M. R., and Rotilio, G., *FEBS Lett.* **263**, 127 (1990).
102. Cole, J. L., Tan, G. O., Yang, E. K., Hodgson, K. O., and Solomon, E. I., *J. Am. Chem. Soc.* **112**, 2243 (1990).
103. Messerschmidt, A., Rossi, A., Ladenstein, R., Huber, R., Bolognesi, M., Gatti, G., Marchesini, A., Petruzzelli, R., and Finazzi-Agrò, A., *J. Mol. Biol.* **206**, 513 (1989).
104. Spiro, T. G., ed., "Molybdenum Enzymes." Wiley (Interscience), New York, 1985.
105. Bray, R. C., *Q. Rev. Biophys.* **21**, 99 (1988).
106. Shah, V. K., and Brill, W. J., *Proc. Natl. Acad. Sci. U.S.A.* **74**, 3249 (1977).
107. Pienkos, P. T., Shah, V. K., and Brill, W. J., *Proc. Natl. Acad. Sci. U.S.A.* **74**, 5468 (1977).
108. Johnson, J. L., Hainline, B. E., and Rajagopalan, K. V., *J. Biol. Chem.* **255**, 1783 (1980).
109. George, G. N., Kipke, C. A., Prince, R. C., Sunde, R. A., Enemark, J. H., and Cramer, S. P., *Biochemistry* **28**, 2075 (1989).
110. Turner, N. A., Bray, R. C., and Diakun, G. P., *Biochem. J.* **260**, 563 (1989).
111. Cramer, S. P., and Hille, R., *J. Am. Chem. Soc.* **107**, 8164 (1985).
112. Hille, R., George, G. N., Eidsness, M. K., and Cramer, S. P., *Inorg. Chem.* **28**, 4018 (1989).
113. George, G. N., and Bray, R. C., *Biochemistry* **27**, 3603 (1988).
114. Cramer, S. P., Solomonson, L. P., Adams, M. W. W., and Mortenson, L. E., *J. Am. Chem. Soc.* **106**, 1467 (1984).
115. George, G. N., Turner, N. A., Bray, R. C., Morpeth, F. F., Boxer, D. H., and Cramer, S. P., *Biochem. J.* **259**, 693 (1989).
116. Cramer, S. P., Hodgson, K. O., Gillum, W. O., and Mortenson, L. E., *J. Am. Chem. Soc.* **100**, 3398 (1978); Cramer, S. P., Gillum, W. O., Hodgson, K. O., Mortenson, L. E., Stiefel, E. I., Chisnell, J. R., Brill, W. J., and Shah, V. K., *ibid.* p. 3814.

117. Conradson, S. D., Burgess, B. K., Newton, W. E., Mortenson, L. E., and Hodgson, K. O., *J. Am. Chem. Soc.* **109**, 7507 (1987).
118. Smith, B. E., Eady, R. R., Lowe, D. J., and Gormal, C., *Biochem. J.* **250**, 299 (1988).
119. Arber, J. M., Dobson, B. R., Eady, R. R., Stevens, P., Hasnain, S. S., Garner, C. D., and Smith, B. E., *Nature (London)* **325**, 372 (1987).
120. Arber, J. M., Dobson, B. R., Eady, R. R., Hasnain, S. S., Garner, C. D., Matsushita, T., Nomura, M., and Smith, B. E., *Biochem. J.* **258**, 733 (1989).
121. George, G. N., Coyle, C. L., Hales, B. J., and Cramer, S. P., *J. Am. Chem. Soc.* **110**, 4057 (1988).
122. Kovacs, J. A., and Holm, R. H., *J. Am. Chem. Soc.* **108**, 340 (1986).
123. Harvey, I., Arber, J. M., Eady, R. R., Smith, B. E., Garner, C. D., and Hasnain, S. S., *Biochem. J.* **266**, 929 (1990).